PHYSICAL REVIEW E **68**, 066116 (2003)

Alternative model of the Antonov problem

L. Velazquez*
Departamento de Física, Universidad de Pinar del Río, Martí 270, Esq. 27 de Noviembre, Pinar del Río, Cuba

F. Guzmán†
Departamento de Física Nuclear, Instituto Superior de Ciencias y Tecnología Nucleares, Carlos III y Luaces, Plaza, La Habana, Cuba
(Received 2 May 2003; published 24 December 2003)

Astrophysical systems will never be in a real thermodynamic equilibrium: they undergo an evaporation process due to the fact that the gravity is not able to confine the particles. Ordinarily, this difficulty is overcome by enclosing the system in a rigid container which avoids the evaporation. We propose an energetic prescription which is able to confine the particles, leading in this way to an alternative version of the Antonov isothermal model which unifies the well-known isothermal and polytropic profiles. Besides the main features of the isothermal sphere model (the existence of the gravitational collapse and the energetic region with a negative specific heat), this alternative model has the advantage that the system size naturally appears as a consequence of the particles' evaporation.

DOI: 10.1103/PhysRevE.68.066116 PACS number(s): 05.70.−a, 05.20.−y

I. INTRODUCTION

Thermodynamical properties of self-gravitating systems are very different from the ones exhibited by the traditional systems. They are typical *nonextensive systems* since they are nonhomogeneous and the total energy is not extensive, which is a consequence of the long-range character of gravitational interaction. They also exhibit energetic regions with a *negative specific heat*, which persist even in the thermodynamic limit [1–8]. That is the reason why the Gibbs canonical ensemble is nonapplicable to the description of self-gravitating systems, since this ensemble is not able to access to those macroscopic states possessing a negative heat capacity. At first glance, the self-gravitating systems could only be described by using the microcanonical ensemble.

Gravitation is not able to confine the particles: it is always possible that some of them have sufficient energy for escaping from the system, so that the self-gravitating systems always undergo an evaporation process. Therefore, they will never be in a real thermodynamic equilibrium. This difficulty is usually avoided by enclosing the system in a rigid container [5–7], which could be justified when the evaporation rate is small and a certain kind of quasistationary state might be reached. There are some approaches which have taken into account this kind of regularization of the long-range singularity of the Newtonian potential in a microcanonical framework [9,10].

The use of a rigid container can be conveniently substituted by imposing the following energetic prescription:

$$\frac{1}{2m}p^2+m\phi(\mathbf{r})\leqslant\epsilon_S<0, \tag{1}$$

where $(1/2m)p^2$ is the kinetic energy of a particle of mass m and $m\phi(\mathbf{r})$ its gravitational potential energy at the point $\mathbf{r}$, ϵ_S being an energy cutoff which is determined from the existence of certain tidal forces. All those particles satisfying condition (1) are confined by gravity; on the contrary, they will be able to escape out from the system if they do not lose their excessive energy. This regularization procedure is characteristic of the Michie-King model for globular clusters [11], which supposes that those stars that gain sufficient velocity through encounters are able to escape or are removed by tidal forces. The main motivation of such a regularization scheme relies on consideration of evaporation effects, and therefore, this regularization procedure is more realistic than the box regularization (the use of a rigid container). The aim of this paper is to develop an alternative model to the standard isothermal sphere model of Antonov [5] based on the consideration of this energetic prescription starting from microcanonical basis.

II. STATISTICAL DESCRIPTION

Let us consider the N-body self-gravitating Hamiltonian system

$$H_N=T_N+U_N=\sum_{k=1}^{N}\frac{1}{2m}\mathbf{p}_k^2-\sum_{j>k=1}^{N}\frac{Gm^2}{|\mathbf{r}_j-\mathbf{r}_k|}. \tag{2}$$

Taking into consideration the above regularization prescription (1), the admissible stages of this system are those in which the kinetic energy of a given particle satisfies the condition

$$\frac{1}{2m}\mathbf{p}_k^2<u_k=m[\phi_S-\phi(\mathbf{r}_k)], \tag{3}$$

$\phi(\mathbf{r}_k)$ being the gravitational potential at the point $\mathbf{r}_k$ where the kth particle is located:

$$\phi(\mathbf{r}_k)=-\sum_{j\neq k}^{N}\frac{Gm^2}{|\mathbf{r}_k-\mathbf{r}_j|}, \tag{4}$$

where we introduce the tidal potential ϕ_S ($\epsilon_S=m\phi_S$).

*Electronic address: luisberis@geo.upr.edu.cu
†Electronic address: guzman@info.isctn.edu.cu

The regularized microcanonical accessible volume W_R is given by

$$W_R=\frac{1}{N!}\int_{X_R}\delta[E-H_N]dX,$$

where X_R is a subspace of the N-body phase space where condition (3) takes place,

$$dX=d^{3N}Rd^{3N}P/(2\pi\hbar)^{3N}=\prod_k\frac{d^3\mathbf{r}_kd^3\mathbf{p}_k}{(2\pi\hbar)^3}$$

being the volume element. The spacial coordinates should be also regularized in order to avoid the short-range divergence of the Newtonian potential, which will be performed below by using the mean-field approximation. This integral is rewritten by using the Fourier representation of the δ function as follows:

$$W_R=\int_{-\infty}^{+\infty}\frac{dk}{2\pi}\exp(zE)\mathcal{Z}_R(z,N), \tag{5}$$

where

$$\mathcal{Z}_R(z,N)=\frac{1}{N!}\int_{X_R}\exp(-zH_N)dX \tag{6}$$

is the canonical partition function with complex argument $z=\beta+ik$, with $\beta\in\mathbb{R}$. Integration by $d^{3N}P$ yields

$$\frac{1}{N!}\int_{\mathbb{R}^{3N}}d^{3N}R\left(\frac{m}{2\pi\hbar^2z}\right)^{3N/2}\exp[-zU_N(R)+\chi(R;z)], \tag{7}$$

$\chi(R;z)$ being

$$\chi(R;z)=\sum_{k=1}^{N}\ln F[\sqrt{zu_k}], \tag{8}$$

where $F(z)$ is defined by

$$F(z)=\mathrm{erf}(z)-\frac{2}{\sqrt{\pi}}z\exp(-z^2) \tag{9}$$

and shown in Fig. 1. The asymptotic behaviors of $F(z)$ are given by

$$F(z)=\begin{cases}\dfrac{4}{3\sqrt{\pi}}z^3+O(z^3) & \text{when } z\to 0,\\ \sim 1, & z\geqslant 2.5.\end{cases} \tag{10}$$

We are interested in describing the large-N limit. This aim can be carried out by using the following procedure: we partition the physical space in cells $\{c_\alpha\}$, $\mathbf{r}_\alpha$ being the positions of their centers. We denoted by $n_\alpha=n(\mathbf{r}_\alpha)$ the number of particles inside the cell at the position $\mathbf{r}_\alpha$. Introducing the density $\rho(\mathbf{r}_\alpha)=n(\mathbf{r}_\alpha)/v_\alpha$, v_α being the volume of the cell c_α, the functions $U_N(R)$ and $\chi(R;z)$ are rewritten by using a *mean-field approximation* as follows:

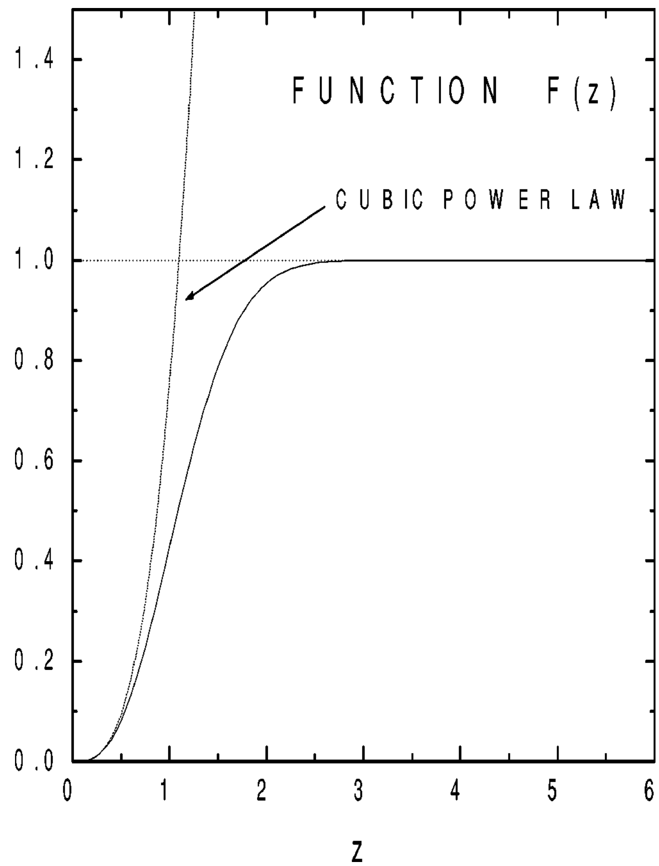

FIG. 1. Representation of the function $F(z)$. Its symptotic behaviors are also shown.

$$U_N(R)\to U[\rho,\phi]=\int_{\mathbb{R}^3}\frac{1}{2}m\rho(\mathbf{r})\phi(\mathbf{r})d^3\mathbf{r}, \tag{11}$$

$$\chi(R;z)\to\chi[\rho,\phi,z]=\int_{\mathbb{R}^3}\rho(\mathbf{r})\ln F(\sqrt{zm[\phi_S-\phi(\mathbf{r})]})d^3\mathbf{r}, \tag{12}$$

$\phi(\mathbf{r})$ being the Newtonian potential for a given ρ profile:

$$\phi(\mathbf{r})=\mathcal{G}[\rho]=-\int_{\mathbb{R}^3}\frac{Gm\rho(\mathbf{r}_1)d^3\mathbf{r}_1}{|\mathbf{r}-\mathbf{r}_1|}, \tag{13}$$

which is the Green solution of the problem

$$\Delta\phi=4\pi G\rho. \tag{14}$$

It is easy to understand that this mean-field approximation acts as a partial regularization procedure for the short-range singularity of the Newtonian potential. The microscopic fluctuations of the Newtonian potential are disregarded in this approximation, since this field is considered constant inside the volume of each cell. Thus the gravity effects on the microscopic picture of each cell are reduced to a truncation of the velocity distribution of the particles. This regularization is partial since it does not avoid the gravitational collapse [5].

Using the partition of the physical space in cells, the integration by $d^{3N}R$ can be approximately given by

$$\frac{1}{N!}\int_{\mathbb{R}^{3N}} d^{3N}R \simeq \sum_{\{n_\alpha\}} \delta_D\left(N-\sum_\alpha n_\alpha\right)\prod_\alpha \frac{v_\alpha^{n_\alpha}}{n_\alpha!}, \quad (15)$$

where

$$\delta_D(k)=\begin{cases}1, & \text{if } k=0,\\ 0, & \text{otherwise,}\end{cases} \quad \text{and} \quad \sum_{\{n_\alpha\}} \equiv \sum_{n_1}\sum_{n_2}\cdots \quad . \quad (16)$$

The following factor can be rephrased in the mean-field approximation as follows:

$$\left(\frac{m}{2\pi\hbar^2 z}\right)^{3N/2}\prod_\alpha \frac{v_\alpha^{n_\alpha}}{n_\alpha!} \to e^{-p_f[\rho,z]}, \quad (17)$$

where

$$p_f[\rho,z]=\int_{\mathbb{R}^3} d^3\mathbf{r}\ \rho(\mathbf{r})\left[\ln \rho(\mathbf{r})-1+\frac{3}{2}\ln\left(\frac{2\pi\hbar^2 z}{m}\right)\right], \quad (18)$$

where the Stirling formula $\ln n! \simeq n \ln n - n$ was used. Finally, we rephrase the summation in the mean-field approximation as follows:

$$\sum_{\{n_\alpha\}} \delta_D\left(N-\sum_\alpha n_\alpha\right) \to \int \mathcal{D}\rho(\mathbf{r})\,\delta\left[N-\int_{\mathbb{R}^3} d^3\mathbf{r}\ \rho(\mathbf{r})\right]. \quad (19)$$

Taking into consideration all approximations introduced above, the canonical partition function (6) is rewritten as

$$\mathcal{Z}_c[z,N]=\int \mathcal{D}\rho(\mathbf{r})\,\delta(N-N[\rho])\exp\{-p_f[\rho,z] - zU[\rho,\phi[\rho]]+\chi[\rho,\phi[\rho];z]\}, \quad (20)$$

$N[\rho]$ being the particle number functional:

$$N[\rho]=\int_{\mathbb{R}^3} d^3\mathbf{r}\ \rho(\mathbf{r}). \quad (21)$$

In order to avoid the complicated ρ dependence of $\phi[\rho]$ in Eq. (20), we introduce the identity

$$\int \mathcal{D}\phi(\mathbf{r})\,\delta\{\phi(\mathbf{r})-\mathcal{G}[\rho]\}=1 \quad (22)$$

in the functional integral (20):

$$\int \mathcal{D}\rho(\mathbf{r})\mathcal{D}\phi(\mathbf{r})\,\delta\{\phi(\mathbf{r})-\mathcal{G}[\rho]\}\,\delta(N-N[\rho]) \times\exp\{-p_f[\rho;z]-zU[\rho,\phi]+\chi[\rho,\phi;z]\}. \quad (23)$$

The δ functions are also conveniently rewritten by using their Fourier representation:

$$\delta\{\phi(\mathbf{r})-\mathcal{G}[\rho]\}\sim\int \mathcal{D}h(\mathbf{r})\exp\left[\int_{\mathbb{R}^3} d^3\mathbf{r}\ J(\mathbf{r})\{\phi(\mathbf{r})-\mathcal{G}[\rho]\}\right], \quad (24)$$

as well as

$$\delta(N-N[\rho])=\int_{-\infty}^{+\infty}\frac{dq}{2\pi}\exp\{z_1(N-N[\rho])\}, \quad (25)$$

$z_1=\mu+iq$ being with $\mu\in\mathbb{R}$; $J(\mathbf{r})=j(\mathbf{r})+ih(\mathbf{r})$, a complex function with $j(\mathbf{r})$ and $h(\mathbf{r})\in\mathbb{R}$. Thus the canonical partition function $\mathcal{Z}_c[z,N]$ is finally expressed as

$$\int_{-\infty}^{+\infty}\frac{dq}{2\pi}\int \mathcal{D}\rho(\mathbf{r})\mathcal{D}\phi(\mathbf{r})\mathcal{D}h(\mathbf{r})\exp\{z_1 N - H[\rho,\phi;z,z_1,J]\}. \quad (26)$$

The functional $H[\rho,\phi;z,z_1,J]$ is given by

$$=p_f[\rho;z]+zU[\rho,\phi]-\chi[\rho,\phi;z]+z_1N[\rho]+K[\phi,\rho,J], \quad (27)$$

$K[\phi,\rho,J]$ being the exponential argument of the expression (24).

The reader may check that when N is scaled as $N\to\alpha N$ and the following quantities are scaled as

$$\rho\to\alpha^2\rho,\quad \mathbf{r}\to\alpha^{-1/3}\mathbf{r},\quad \phi\to\alpha^{4/3}\phi,$$
$$z\to\alpha^{-4/3}z,\quad z_1\to z_1,\quad J\to\alpha^{2/3}J, \quad (28)$$

all terms in Eq. (27) scale proportional to α, and therefore

$$H[\rho,\phi;z,z_1,J]\to\alpha H[\rho,\phi;z,z_1,J]. \quad (29)$$

The thermodynamic limit is carried out tending α to infinity, $\alpha\to\infty$. Thus, we can estimate $\mathcal{Z}_c[z,N]$ for N large by using the *steepest decent method*. The Planck potential $\mathcal{P}(\beta,N)=-\ln \mathcal{Z}_c[\beta,N]$ is thus obtained as follows:

$$\mathcal{P}[\beta,N]\simeq-\max_{\rho,\phi}\left\{\min_{\mu,j}[\mu N-H[\rho,\phi;\beta,\mu,j]]\right\}. \quad (30)$$

where the stationary conditions

$$\frac{\delta H}{\delta\rho}=\frac{\delta H}{\delta\phi}=\frac{\delta H}{\delta j}=\frac{\delta H}{\delta\mu}-N=0 \quad (31)$$

lead to the relations

$$\rho=\left(\frac{m}{2\pi\hbar^2\beta}\right)^{3/2}\exp\left[-\mu-\frac{1}{2}\beta m\phi+\mathcal{G}[j]\right] \times F[\sqrt{\beta m[\phi_S-\phi]}], \quad (32)$$

$$j=-\frac{1}{2}\beta m\rho+\rho\partial_\phi \ln F[\sqrt{\beta m[\phi_S-\phi]}], \quad (33)$$

$$\phi = \mathcal{G}[\rho] \quad \text{and} \quad N = N[\rho]. \tag{34}$$

The relations (32) and (33) define the state equation, and the relations (34) establish the Newtonian potential ϕ for a given ρ profile as well as the normalization constrain for the number of particles. The relation (32) is conveniently rewritten by using Eq. (33) as follows:

$$\rho = N(\beta,\mu)\exp[\Phi + C]F(\Phi^{1/2}), \tag{35}$$

where $\Phi = \beta m[\phi_S - \phi]$ and

$$N(\beta,\mu) = (m/2\pi\hbar^2\beta)^{3/2}\exp(-\mu - \beta m\phi_S),$$

C being a new function, which is given by

$$C = -\beta m \mathcal{G}[\rho\partial_\Phi \ln F(\Phi^{1/2})]. \tag{36}$$

It is not difficult to show that the Planck potential is given by

$$\mathcal{P}(\beta,N) = -\left(1 + \mu + \frac{1}{2}\beta m\phi_S\right)N + \int_{\mathbb{R}^3} d^3\mathbf{r}\ \rho\left(\frac{1}{2}\Phi + C\right). \tag{37}$$

The Boltzmann entropy can be estimated by using the steepest decent method as follows:

$$S_B(E,N) \simeq \min_\beta[\beta E - \mathcal{P}[\beta,N]], \tag{38}$$

$E[\beta,\rho,\phi]$ being the energy functional,

$$E[\beta,\rho,\phi] = \int_{\mathbb{R}^3} d^3\mathbf{r}[3 - \Phi\partial_\Phi \ln F(\Phi^{1/2})]\frac{1}{2\beta}\rho + \frac{1}{2}m\rho\phi. \tag{39}$$

It can be easily seen that the quantity

$$\epsilon(\beta,\Phi) = [3 - \Phi\partial_\Phi \ln F(\Phi^{1/2})]\frac{1}{2\beta} \tag{40}$$

represents the *kinetic energy per particle* at a given point of the self-gravitating system. Note that ρ vanishes when Φ tends to zero in Eq. (35), so that the particle distribution has been *regularized*. This state equation differs from the one obtained in the isothermal model by the presence of the truncation function $F(\Phi^{1/2})$ as well as the *driving function C*. Although C naturally appears in our derivation, its existence is closely related with the modification provoked in the microscopic picture of the system by the evaporation. An example of this affirmation is the deviation of the Maxwell distribution along the system, which can be noted in the kinetic energy per particle $\epsilon(\beta, \Phi)$ [Eq. (40)]. A naive energy truncation of the *Maxwell-Boltzmann distribution*,

$$\omega_{\mathrm{MB}} = C_0 \exp\left[-\beta\left(\frac{1}{2m}p^2 + m\phi\right)\right], \tag{41}$$

leads to the state function

$$\rho \sim \exp[\Phi]F(\Phi^{1/2}), \tag{42}$$

but here the driving function C does not appear.

According to the scaling laws (28), this astrophysical model obeys the following thermodynamic limit:

$$N \to \infty, \quad \text{keeping constant } \frac{E}{N^{7/3}} \quad \text{and} \quad LN^{1/3}, \tag{43}$$

L being the characteristic system size. This thermodynamic limit was obtained in Ref. [12] for the self-gravitating fermion model. The reader may be surprised by the N dependence of the characteristic system size L. However, there is nothing strange in this behavior since the self-gravitating gas is constituted by *punctual* particles, and therefore, this model system can be reduced to a point in the thermodynamic limit $N \to \infty$.

It is easy to understand that this is an asymptotical behavior which disappears when the particles' size and/or the relativistic effects are taken into account. It means that there should exist a superior limit of N in which these N dependences of the energy and system size become invalid, and therefore, the self-gravitating nonrelativistic gas model is inapplicable for describing the thermodynamical properties of such massive astrophysical systems.

It is interesting to analyze the asymptotic behavior of the particles density state function $\rho(\Phi;\ \beta,\ \mu)$. According to the asymptotic behaviors (10) of the function $F(z)$, the state equation (35) becomes in the *isothermal distribution* when $\sqrt{\Phi} > 2.5$:

$$\rho \propto \exp[\Phi], \tag{44}$$

which is characteristic of the inner regions of the system (the core). At local level, the particles velocities obey to a Maxwell distribution, where the kinetic energy per particle, Eq. (40), is given by $3/2\beta$. When we move from the inner regions towards the outer ones, the kinetic energy per particle decreases until zero, being this approximately given by $\epsilon \simeq 3\Phi/5\beta$. There the particles velocities obey a *uniform distribution*, and so the state equation in the halo obeys a *polytropic distribution*

$$\rho \propto \frac{4}{3\sqrt{\pi}}\Phi^{3/2}. \tag{45}$$

All these behaviors appear as consequence of the high-energy cutoff (3) in the Maxwell distribution for the kinetic energy $f(k) = 2\pi^{-1/2}k^{1/2}\exp(-k)$ $(k = \beta\mathbf{p}^2/2m)$, which is shown in Fig. 2. Note that the cutoff value of k is equal to Φ. In the inner regions where $\sqrt{\Phi} > 2.5$, this energy cutoff is unimportant because it is located in the tail of the distribution. However, it modifies considerably the character of the state function for ρ in the halo due to the fact that it is located before the pick. The particles density ρ will obey the polytropic dependence (45) throughout the whole system volume when Φ is also small in the inner regions.

Thus the consideration of the energetic prescription (1) always leads to the existence of a polytropic halo, where the system core can be isothermal or polytropic, according to the values of the function Φ in the inner regions of the system. Due to the general properties of the spherical solutions with

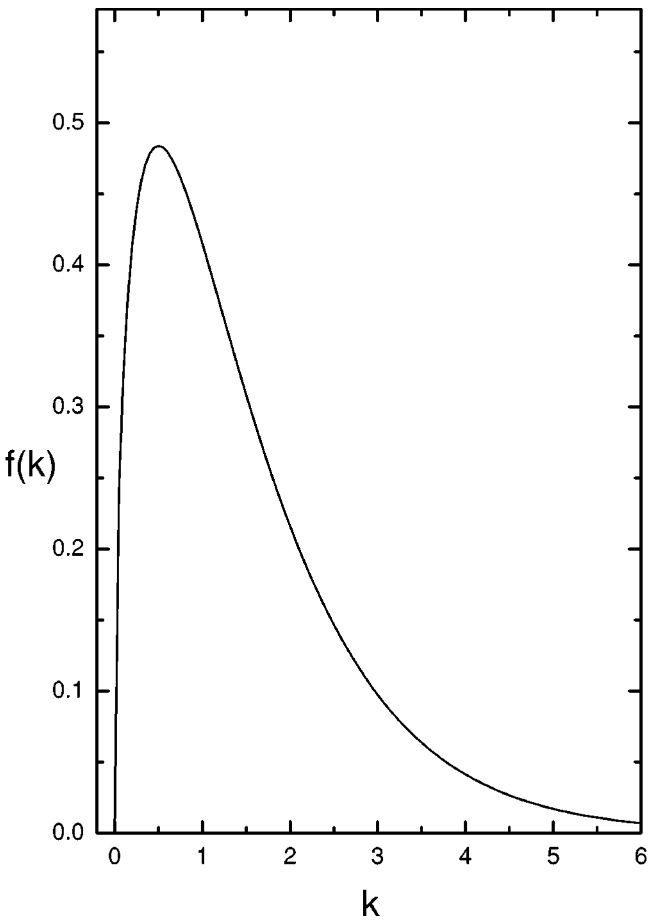

FIG. 2. Maxwell distribution for the kinetic energy. The character of the state function for the particles' density ρ depends on the localization of the energy cuttoff Φ.

a polytropic profile, the particles' density will *vanish* at a finite radio $R_{\rm tidal}$, which can be identified with the characteristic size of the system. This radio is related to the tidal potential ϕ_S throughout the relation

$$\phi_S = -\frac{GM}{R_{\rm tidal}}, \tag{46}$$

M being the system total mass. Thus the characteristic size of the system is *determined* by the tidal interactions.

III. NUMERICAL STUDY

In order to perform a numerical study of the equations obtained in the previous section, we express the energy in units of $E_0 = GM^2/R_{\rm tidal}$ and the length in units of the system size $R_{\rm tidal}$ and the mass in units of M. It is not difficult to show that the functions Φ and C obey the following structure equations:

$$\Delta_r \Phi = -4\pi F_1(\Psi,\Phi), \quad \Delta_r \Psi = -4\pi F_2(\Psi,\Phi), \tag{47}$$

where $\Delta_r u = r^{-2}\partial_r(r^2 \partial_r u)$ is the radial part of the Laplace operator, the functions $F_1(\Psi,\Phi)$ and $F_2(\Psi,\Phi)$ being defined by

$$F_1(\Psi,\Phi) = \exp(\Psi+\Phi) F(\Phi^{1/2}),$$

$$F_2(\Psi,\Phi) = \frac{2}{\sqrt{\pi}} \exp(\Psi)\Phi^{1/2}. \tag{48}$$

In the expressions above the function $\Psi = C + \ln \mathcal{K}(\beta,\mu)$, with $\mathcal{K}(\beta,\mu) = \beta^{1/2} \exp(-\mu+\beta)$. The solutions of the nonlinear system (47) satisfy the following conditions at the surface:

$$\Phi(1) = 0, \quad \Phi'(1) = -\beta, \quad C(1) = -C'(1), \tag{49}$$

which are derived from the boundary conditions of the Green solutions (13).

The solution can be obtained from the imposition of the following boundary conditions at the origin:

$$\Delta(0) = \Phi_0 > 0, \tag{50}$$

$$\Psi(0) = \Psi(\Phi_0), \tag{51}$$

where the value of $\Psi(0)$ depends on the parameter Φ_0 because Φ must vanish when $r=1$. This situation can be overcome by redefining the problem as follows:

$$\Psi(r) = \psi(\xi) + 2 \ln R_m, \quad \Phi(r) = \varphi(\xi), \tag{52}$$

$\{\varphi(\xi),\psi(\xi)\}$ being the solution of Eq. (47) whose boundary conditions are given by

$$\varphi(0) = \Phi_0 > 0, \quad \varphi'(0) = 0, \quad \psi(0) = 0, \quad \psi'(0) = 0, \tag{53}$$

where ξ is related with r throughout the relation

$$r = \xi / R_m, \tag{54}$$

R_m being the radio at which φ vanishes $[\varphi(R_m) = 0]$.

The canonical parameter β and μ are obtained from the relations

$$R_m \partial_\xi \varphi(R_m) = -\beta = -\beta(\Phi_0), \tag{55}$$

$$\psi(R_m) + R_m \partial_\xi \psi(R_m) = -h, \tag{56}$$

where $h = h(\Phi_0) \equiv -\ln[\mathcal{K}(\beta,\mu)/R_m^2]$, which allow us to express μ as a function of Φ_0:

$$\mu = h + \beta - \frac{1}{2} \ln \beta - 2 \ln R_m. \tag{57}$$

Taking into consideration Eqs. (39) and (37), the total energy and Planck potential per particle are rewritten as follows:

$$\epsilon(\Phi_0) = \frac{3}{2\beta} - \frac{1}{2} - \frac{1}{\beta^2 R_m} h_1(\Phi_0), \tag{58}$$

$$\mathcal{P}(\Phi_0) = -1 - \mu + \frac{1}{2}\beta + h(\Phi_0) + \frac{1}{\beta R_m} h_2(\Phi_0), \tag{59}$$

where

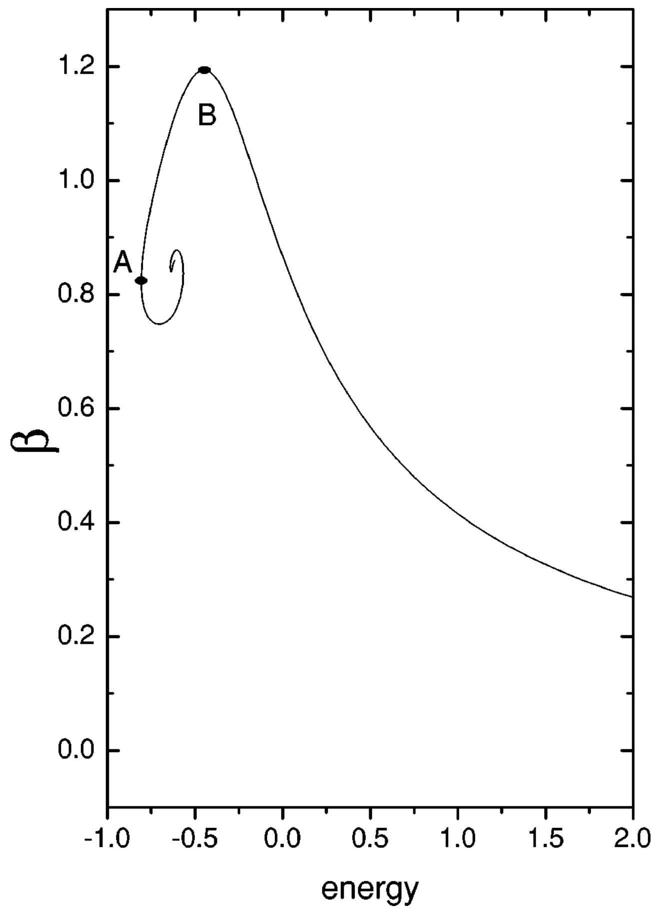

FIG. 3. The alternative model exhibits the main features of the isothermal model of Antonov. It adopted the characteristic units assumed at the beginning of Sec. III for all figures of the present section.

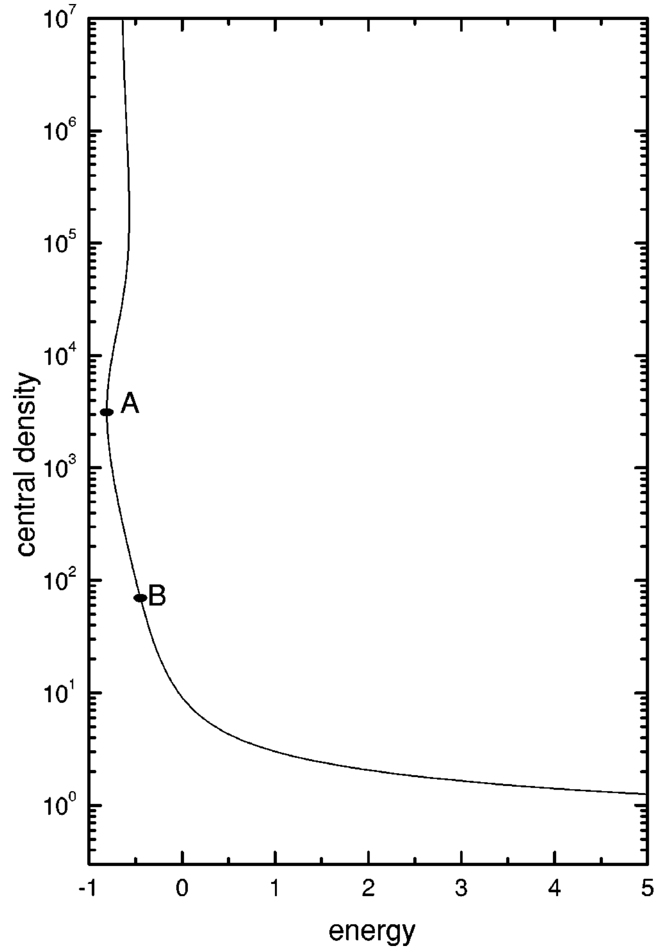

FIG. 4. Central density vs energy: this dependence shows the existence of the gravitational collapse for $\epsilon<\epsilon_A$.

$$h_1(\Phi_0)=\int_0^{R_m}4\pi\xi^2 d\xi\,\frac{1}{2}\,\varphi[F_1(\psi,\varphi)+F_2(\psi,\varphi)], \tag{60}$$

$$h_2(\Phi_0)=\int_0^{R_m}4\pi\xi^2\,d\xi\,F_1(\psi,\varphi)\left(\frac{1}{2}\,\varphi+\psi\right). \tag{61}$$

IV. RESULTS AND DISCUSSIONS

Figures 3 and 4 show respectively the caloric curve and the central density of the model. These dependences evidence that this model system exhibits the main features of the Antonov isothermal model: the existence of a negative specific heat when $\epsilon_A<\epsilon<\epsilon_B$ and gravitational collapse for $\epsilon<\epsilon_A$, where the central density grows towards infinity and the system develops a core-halo structure, where $\epsilon_A=-0.806$ and $\epsilon_B=-0.446$.

This conclusion is supported by the analysis of the thermodynamical potentials of the model: the entropy in the microcanonical ensemble, in Fig. 5, and the Planck potential in the canonical ensemble, in Fig. 6. Figure 5 shows that the points of the superior branch of the caloric curve 3 correspond to equilibrium configuration while the others represent unstable saddle points. No equilibrium states exist when $\epsilon<\epsilon_A$.

On the other hand, Fig. 6 evidences that the canonical ensemble can access only those equilibrium states belonging to the interval $0<\beta<\beta_B$ (with $\epsilon>\epsilon_B$), where $\beta_B=1.193$. The energetic region $\epsilon_A<\epsilon<\epsilon_B$ is invisible for the canonical description due to the negativity of the heat capacity. No equilibrium states exist for $\beta>\beta_B$. This fact evidences the existence of a gravitational collapse in the canonical ensemble beyond the critical point β_B, which is usually referred as an *isothermal collapse* [13].

The Gibbs argument—the equilibrium of a subsystem with a thermal bath—is nonapplicable to this situation because of no reasonable thermal bath exits for the astrophysical systems. Therefore, the isothermal catastrophe is not a phenomenon with physical relevance since it can be never obtained in nature: the consideration of a thermal bath in the astrophysical system is outside of context. A different significance possesses the gravothermal catastrophe. The gravitational collapse is the main engine of structuration in astrophysics and it concerns almost all scales of the universe: the formation of planetesimals in the solar nebula, the formation of stars, the fractal nature of the interstellar medium, the evolution of globular clusters and galaxies, and the formation of galactic clusters in cosmology [13].

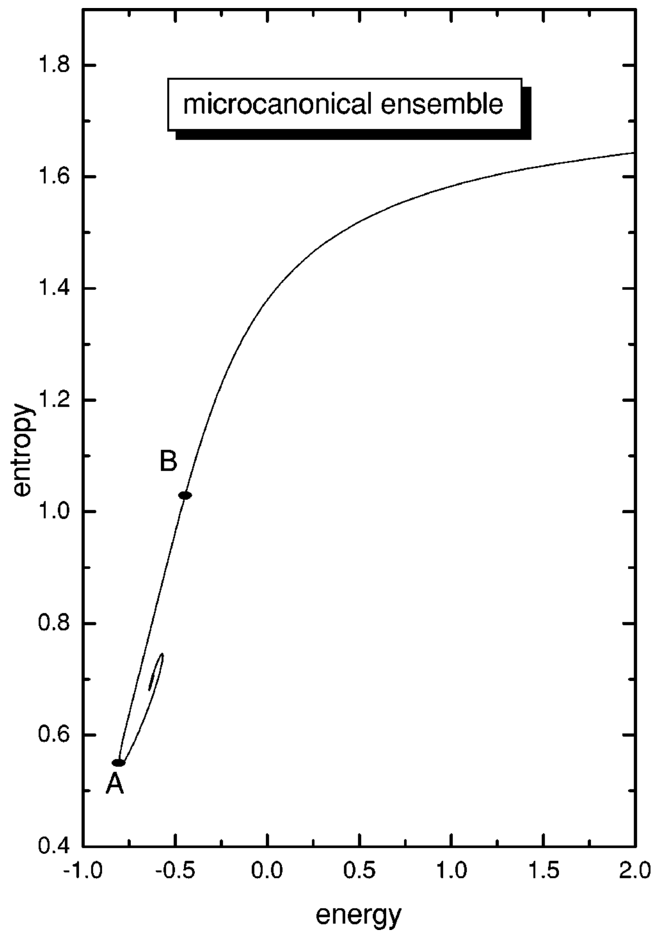

FIG. 5. Entropy vs energy: equilibrium configurations exit only for $\epsilon > \epsilon_A$.

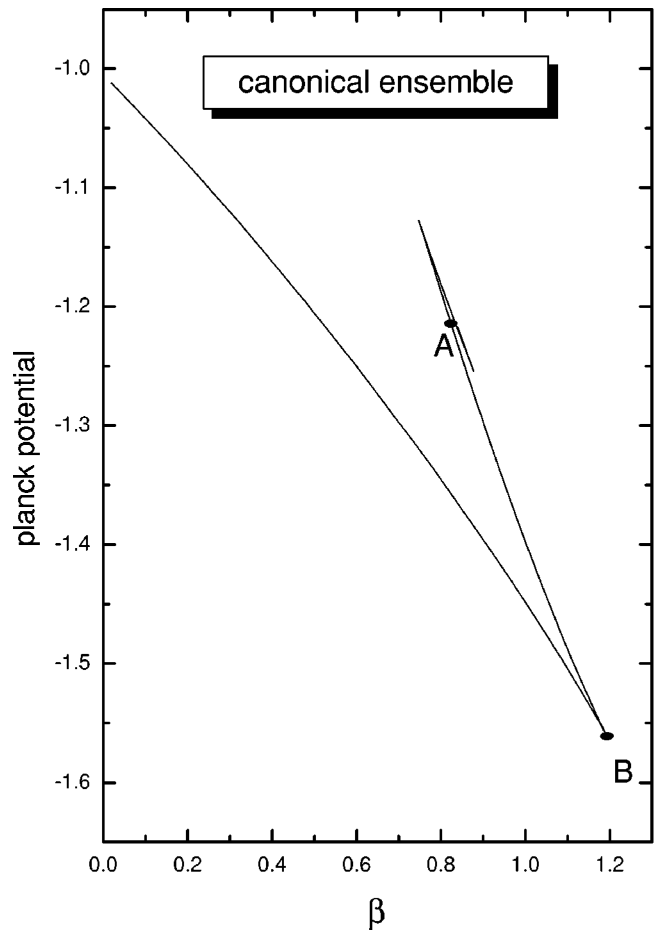

FIG. 6. Planck potential vs inverse temperature: the canonical ensemble accesses only to those equilibrium stages with $\beta < \beta_B$ ($\epsilon > \epsilon_B$).

Let us now carry out a comparative study between the isothermal model and this alternative one. As already mentioned, the only difference between these approaches relies on the regularization prescription of the long-range singularity of the self-gravitating gas: the isothermal model avoids particle evaporation by using a rigid container, while the present model takes into account the effects of this evaporation by truncating the kinetic energy distribution function. This study is carried out by considering a spherical container in the isothermal model with a linear dimension $R = R_{\mathrm{tidal}}$.

Figure 7 shows the caloric curves of these models. In spite of the qualitative similarity of these dependences, the alternative model is able to describe an additional energetic range from -0.806 to -0.335, but the isothermal model describes equilibrium configurations belonging to the interval $1.193 < \beta < 2.518$, which are cooler than the ones described by using the first model.

A second difference is evidenced in regard to the central density versus energy dependence, which is shown in Fig. 8. The central density at the critical energy of the gravitational collapse is much greater in the alternative model than the isothermal one, and this qualitative relationship seems to be applicable to the whole energetic range.

Figure 9 shows two interesting observables: the radio in which the system exhibits an isothermal behavior, R_{ic}, and the mass content enclosed inside, M_{ic}. These quantities characterize the size and mass of the isothermal core. The reader may observe that the isothermal core contains at the critical energy of the gravitational collapse half of the system total mass inside $\sim 1\%$ of the system volume. On the other hand, it is interesting to note that this isothermal core disappears at $\epsilon^* \simeq -0.066$.

The quantitative differences in the thermodynamical description between these models seem to be explained by the following reasonings. Most of the energy contribution to the total energy comes from the isothermal core. The contribution of the gravitational potential energy is dominant in the core due to the high mass concentration enclosed inside this region, where, moreover, the Newtonian potential exhibits its highest values. Outside the isothermal core, the kinetic energy contribution decreases considerably as a consequence of the deviation from the isothermal character of the microscopic particle distribution function due to evaporation.

These arguments can be rephrased as follows: in the isothermal region, where $-0.806 < \epsilon < -0.066$, the present model behaves as an isothermal model with a characteristic size equal to the size of the isothermal core. Since the relevant canonical variables in the isothermal model is $\eta = \beta G M / R$ [5,13], a rough estimation of the maximal value $\beta_{\max} = \beta_B$ in which the isothermal collapse takes places is given by

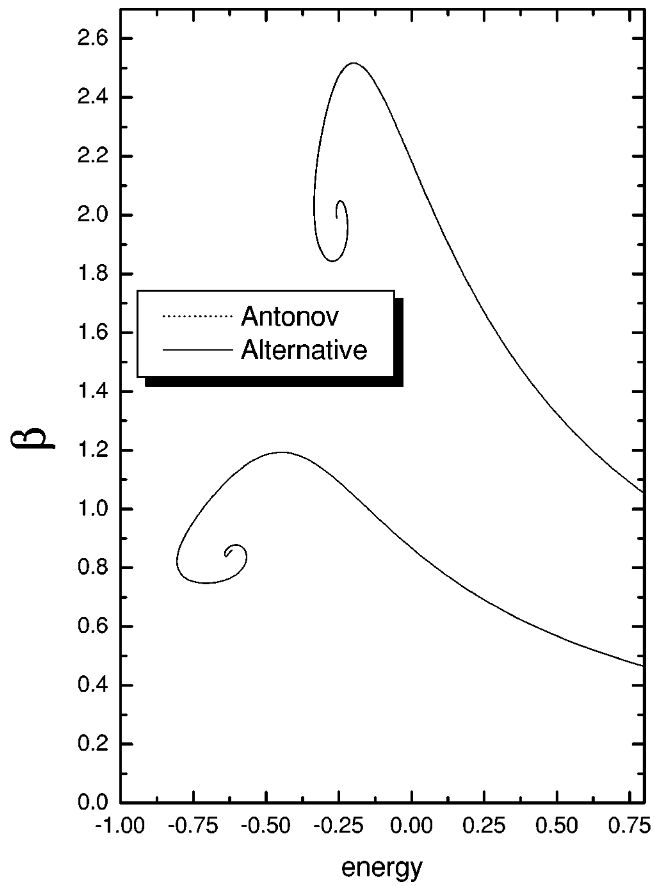

FIG. 7. The caloric curves: The figure shows the comparison between the two models.

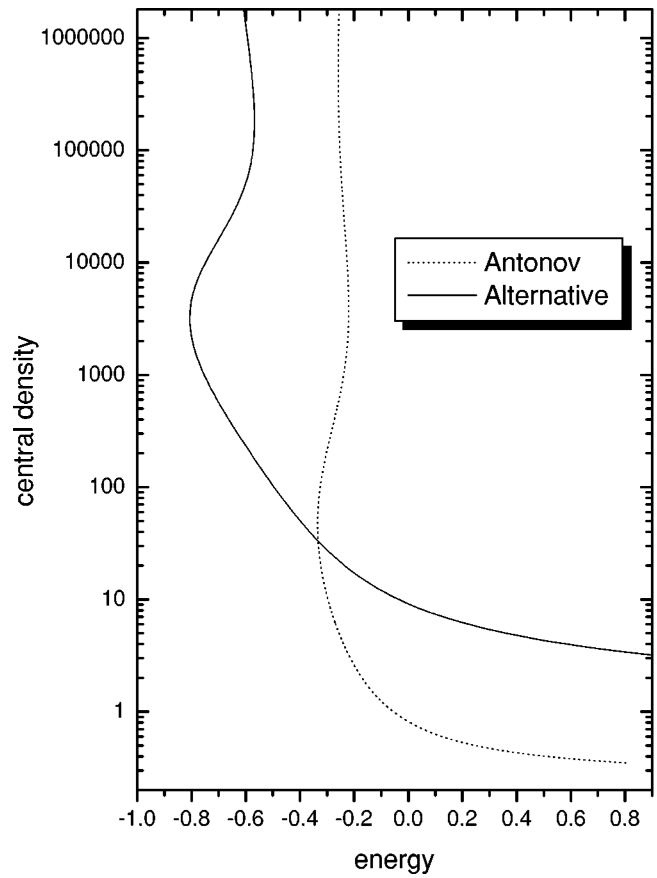

FIG. 8. The central density vs energy. The central density is much greater in this alternative version of the Antonov problem.

$$\beta_B \approx \frac{R_{ic}}{M_{ic}} \beta_{max}^{isoth}. \tag{62}$$

By using the characteristics values $R_{ic} \approx 0.2$, $M_{ic} \approx 0.5$, and $\beta_{max}^{isoth} \approx 2.5$ (obtained from the isothermal model), the formula (62) gives a fairly good estimation of $\beta_B \approx 1$ ($\beta_B = 1.193$).

The main difference between these models is in regard to the character of the equilibrium profiles in the high-energy region with $\epsilon > 0$. As already discussed, the isothermal core has disappeared in this energetic region and the equilibrium configurations of the system are essentially polytropic, while the isothermal model leads to a uniform distribution of the particles throughout the volume of the rigid container.

In this case, the structure equations (47) become in a *quasipolytropic model*

$$\Delta\Phi = -4\pi \exp(\Psi) \frac{4}{3\sqrt{\pi}} \Phi^{3/2},$$

$$\Delta\Psi = -4\pi \exp(\Psi) \frac{2}{\sqrt{\pi}} \Phi^{1/2}, \tag{63}$$

which exhibits the same fractal characteristics of a polytropic model with polytropic index $\gamma = \frac{5}{3}$. This polytropic index characterizes an adiabatic process of the ideal gas of particles, which is in our case the evaporation of the system in the vacuum. However, this equation system is not equivalent to the polytropic model due to the presence of the driving function C. This purely polytropic profile is obtained by disregarding the second equation and setting $\Psi \equiv 0$ in the first one.

Let us finalize our discussion by carrying out a comparative study among the equilibrium profiles obtained from the alternative model with the well-known isothermal and polytropic profiles. These equilibrium profiles are shown in Fig. 10. Equilibrium profiles A and C were obtained from the alternative model: profile A corresponds to an equilibrium configuration possessing an isothermal core, while C is a quasipolytropic equilibrium profile. Profiles B and D correspond, respectively, to isothermal and polytropic configurations. The reader can note that the alternative model profiles differ essentially in regard to the existence of the isothermal core, since no qualitative differences are evidenced in the halo structure. On the other hand, these results suggest that a system undergoing an evaporation process concentrates their particles in the inner regions more than what the isothermal or the polytropic models predict.

V. CONCLUSIONS

As already shown in the present paper, the consideration of the energetic prescription (1) leads to an alternative version of the Antonov problem. This model, besides exhibiting the main features of the isothermal model—the gravitational

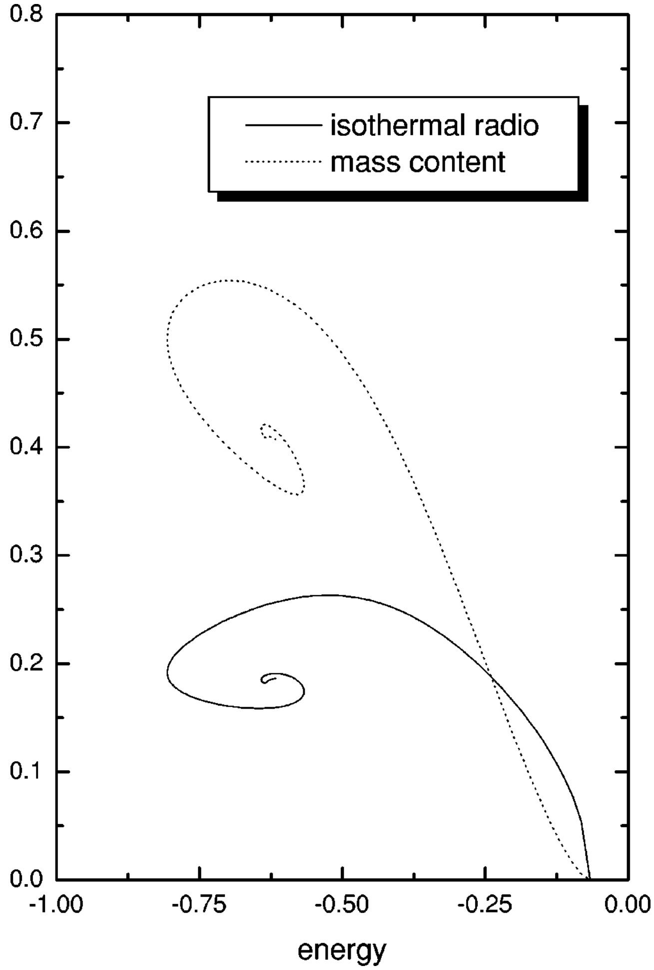

FIG. 9. Isothermal core radio and its mass content in the alternative model.

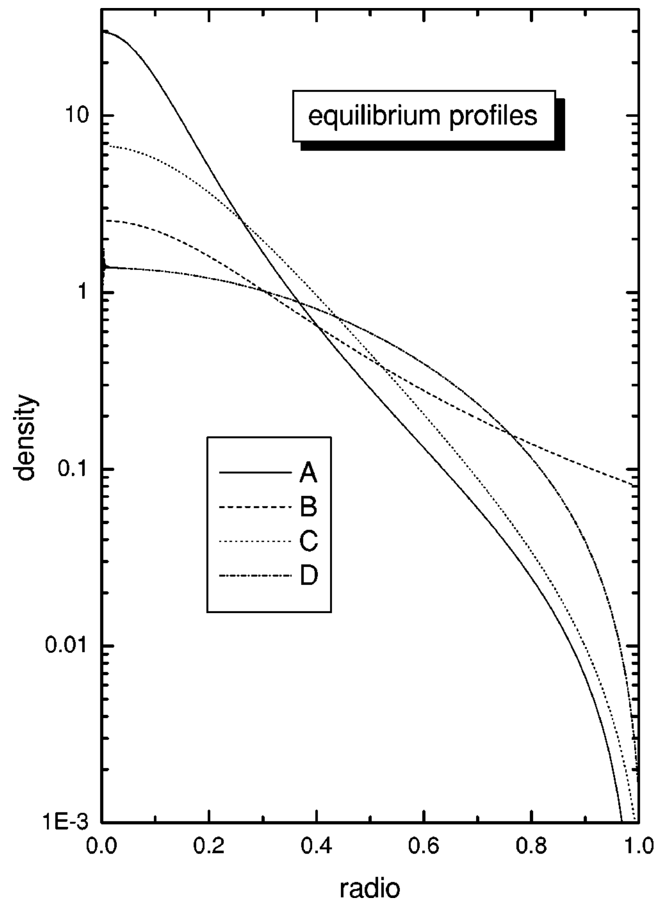

FIG. 10. Comparison among the equilibrium profiles: alternative model with an isothermal core (curve *A*), isothermal profile (curve *B*), alternative model with a quasipolytropic profile (curve *C*), and purely polytropic profile (curve *D*).

collapse and the energetic region with a negative specific heat—has the advantage that the system size naturally appears as a consequence of the particles evaporation. There is no need for enclosing the system in a rigid container in order to avoid the long-range singularity of the Newtonian potential because this regularization procedure is sufficient to access finite equilibrium configurations.

It is remarkable that the present approach unifies the well-known isothermal and polytropic equilibrium profiles. As already mentioned, the equilibrium profiles derived from this alternative model differ essentially in regard to the existence of the isothermal core, since no qualitative differences are evidenced in the halo structure. A comparative study of the equilibrium ρ profiles suggests that a system undergoing an evaporation process concentrates the particles in the inner regions more than what is predicted by the isothermal or polytropic model.

There are many open questions in the study of this model system by using this kind of regularization scheme, for example, the dynamical aspects: Which is the influence of the particles' evaporation in the system dynamical evolution? How could this dynamical description be performed by preserving this energetic prescription? Further studies should clarify these questions. The present study is carried out by considering that the evaporation rate is small enough in order to ensure that the system reaches a quasistationary state. This assumption is satisfied by the globular clusters, since the relaxation time t_{relax} in them differs considerably from the evaporation time t_{evap}, $t_{\mathrm{relax}} \ll t_{\mathrm{evap}}$ (see Ref. [14]). The dynamical approach could be developed by considering that the system evolves slowly throughout these quasistationary states.

[1] T. Padmanabhan, Phys. Rep. **188**, 285 (1990).
[2] M. Kiessling, J. Stat. Phys. **55**, 203 (1989).
[3] D. Ruelle, Helv. Phys. Acta **36**, 183 (1963); M. E. Fisher, Arch. Ration. Mech. Anal. **17**, 377 (1964).
[4] J. van der Linden, Physica (Amsterdam) **32**, 642 (1966); **38**, 173 (1968); J. van der Linden and P. Mazur, *ibid.* **36**, 491 (1967).
[5] V. A. Antonov, Vestn. Leningr. Univ., Ser. 3: Biol. **7**, 135

(1962).
[6] D. Lynden-Bell and R. Wood, Mon. Not. R. Astron. Soc. **138**, 495 (1968); D. Lynden-Bell, *ibid.* **136**, 101 (1967).
[7] D. Lynden-Bell and R. Wood, Mon. Not. R. Astron. Soc. **138**, 495 (1968).
[8] W. Thirring, Z. Phys. **235**, 339 (1970).
[9] E. V. Votyakov, H. I. Hidmi, A. De Martino, and D. H. E. Gross, Phys. Rev. Lett. **89**, 031101 (2002).
[10] H. J. de Vega and N. Sanchez, Phys. Lett. B **490**, 180 (2000); Nucl. Phys. B **625**, 409 (2002); **625**, 460 (2002).
[11] J. Binney and S. Tremaine, *Galactic Dynamics*, Princeton Series in Astrophysics (Princeton University Press, Princeton, 1987).
[12] P. H. Chavanis, Phys. Rev. E **65**, 056123 (2002); P. H. Chavanis and I. Ispolatov, *ibid.* **66**, 036109 (2002).
[13] P. H. Chavanis, C. Rosier, and C. Sire, e-print cond-mat/0107345.
[14] M. J. Benacquista, www.livingreviews.org/Articles/Volume5/2002-2benacquista